ADVANCED MATERIALS

DOI: 10.1002/adma.200601354

Micropatterned Porous-Silicon Bragg Mirrors by Dry-Removal Soft Lithography**

By *Daniel J. Gargas*, *Ovidiu Muresan*, *Donald J. Sirbuly*, and *Steven K. Buratto**

Multilayer structures of nanoporous silicon have garnered significant interest as components of optical and sensing devices due to their low cost, ease of fabrication, and large-scale synthesis.[1–4] Porous silicon (PSi) layer formation via electrochemical etching offers a simple platform to tune the refractive index (i.e., porosity) of stacked layers, which has led to a host of applications based on the optical properties of thin PSi layers. Recent studies have demonstrated the application of PSi superlattices in chemical sensors,[5–7] waveguides,[8] interference filters,[9] distributed Bragg reflectors, and optical microcavities.[10–12] Due to the high surface area of their porous structure (200–500 $m^2 cm^{-3}$),[6] PSi Bragg reflectors (Bragg mirrors) have shown great potential as biological and chemical sensors based on optical reflectance spectroscopy.[13–16] Such chemical sensors function via infiltration of a chemical species into the pore structure, which alters the effective refractive index of the dielectric medium. The shift in the Bragg wavelength (i.e., rejected light) caused by the index change can be probed using simple reflectance spectroscopy or colorimetry. Since the inclusion of chemicals into the porous layers is reversible, the films can be cycled through multiple detection runs without additional preparation steps.

A significant challenge faced in integrating PSi Bragg mirrors into miniature optical devices is the reduction of functional PSi multilayer structures to the micro- and nanometer scales. Active length scales below one micrometer would be ideal for a multiplex sensor based on PSi, which would require multiple chemical-specific PSi Bragg mirrors on a single platform. To date, there exist several techniques to produce spatially confined PSi microstructures either by photolithography or electron-beam lithography, however, there have been no reports on PSi superlattices fabricated to micro- or nanoscale dimensions. Recent work by Sailor and co-workers has shown that PSi photonic crystals with dimensions less than 1 mm^2 can be produced using a lithographically patterned photoresist.[17,18] This technique, although effective, requires additional processing steps for each sample. Therefore it is advantageous to develop simple one-step patterning techniques that retain cost-effectiveness and minimize preparation times.

Microcontact printing, a subfield of soft lithography, is a simple and inexpensive method of fabricating relatively large quantities of microstructured materials.[19] This method utilizes a microprinting technique whereby thin-film structures are patterned on a micrometer scale by direct lift-off.[20,21] Previous efforts in our group have demonstrated the effectiveness of PSi pattern formation by dry-removal soft lithography that uses nothing more than a clean polydimethylsiloxane (PDMS) elastomer stamp.[22,23] Furthermore, this stamping procedure can be followed with an additional transfer step that deposits patterned microstructures from the PDMS stamp onto a flexible polymer film.[22]

In this communication, we build upon previous work by showing that our dry-removal technique can be used to produce ordered arrays of freestanding PSi multilayers without damaging the optical integrity of the film. This method allows relatively large-scale production of uniform nanostructures of optically tunable PSi Bragg mirrors in a variety of shapes and dimensions. In addition, we demonstrate the chemical-sensing capability of a PSi Bragg mirror with various levels of exposure to an infiltrating polymer, as well as the reversible detection of a volatile substance within our micropatterned photonic structures.

Micrometer-sized PSi Bragg mirrors were fabricated by direct contact and subsequent lift-off using a patterned PDMS-elastomer stamp. A schematic representation of the patterning procedure is illustrated in Figure 1. A patterned PDMS stamp was brought into contact with a PSi Bragg mirror composed of alternating layers of high and low porosity. After 5–10 min of slight applied pressure (a 50 g weight), the stamp was peeled away, resulting in a negative pattern formation of the stamp. Regions where the stamp touched the PSi film were subsequently removed from the surface without damaging the material that resided under the structured side of the stamp (Fig. 1C). A contrast-enhanced optical image revealed green, reflecting 100 μm diameter discs affixed to a Si substrate (Fig. 1D). A secondary step was employed to transfer the removed PSi Bragg mirror pattern to a freestanding polymer film. To ensure proper transfer, a solution of the hydrophobic polymer poly[(vinyl butyral)-*co*-(vinyl alcohol)-*co*-(vinyl acetate)] (PVB) in ethanol was drop-cast directly on the stamp surface and allowed to cure (Fig. 1F). After curing, the polymer was gently peeled from the stamp resulting in complete transfer of the PSi microstructures to the mechanically

[*] Prof. S. K. Buratto, D. J. Gargas, O. Muresan, Dr. D. J. Sirbuly[+]
Department of Chemistry and Biochemistry
University of California Santa Barbara
Santa Barbara, CA 93106-9510 (USA)
E-mail: Buratto@chem.ucsb.edu

[+] Present address: Chemistry and Materials Science Directorate, Lawrence Livermore National Laboratory, Livermore, CA 94550, USA.

[**] This work was supported by the National Science Foundation (CHE-0316231).

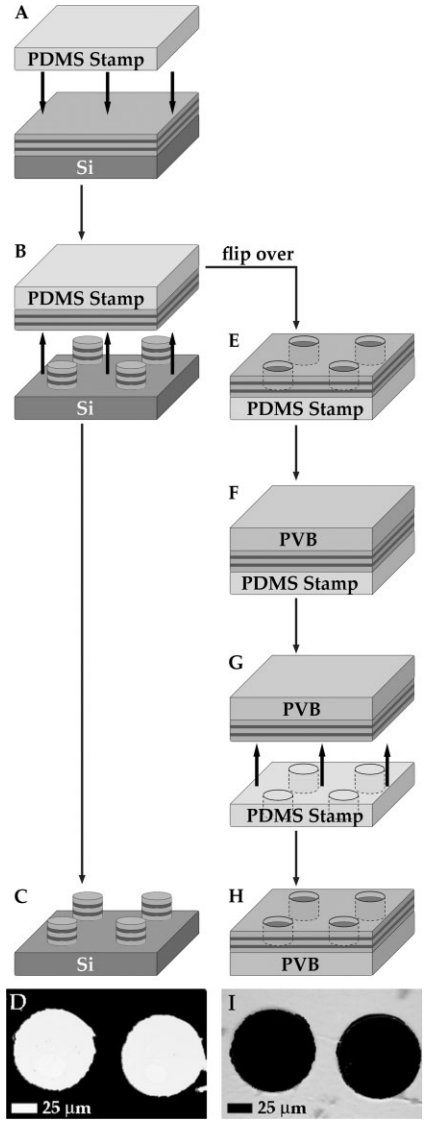

Figure 1. Scheme for fabricating patterned PSi Bragg mirrors by dry-removal soft lithography. A) A patterned PDMS stamp was brought into contact with a PSi Bragg mirror, which consists of alternating layers of high- and low-porosity Si. B) PSi regions in direct contact with the stamp were removed from the Si substrate when the stamp was peeled away, producing a patterned Bragg mirror, shown in (C). D) A contrast-enhanced optical image showing 100 μm diameter PSi Bragg mirror discs patterned on the Si substrate. E) The inverse pattern of the PSi Bragg mirror that was transferred to the PDMS stamp is coated with a PVB polymer film, as seen in (F). G) Peeling the polymer film from the PDMS stamp results in a patterned PSi Bragg mirror on a flexible polymer film, shown in (H). I) A contrast-enhanced optical image showing the PSi Bragg mirror inverse pattern on a flexible polymer film.

flexible, optically transparent polymer film (Fig. 1H). The contrast-enhanced optical image in Figure 1I shows the free-standing PSi Bragg mirrors patterned on a flexible polymer support. Figure 1D and I demonstrates the capacity to transfer a micropatterned PSi Bragg mirror to a flexible polymer film while maintaining its optical properties. This technique has great potential in flexible display devices. Furthermore, the shape and design of the PSi Bragg mirror micropattern on the Si substrate was simply the inverse pattern of the PDMS stamp, whereas the PSi Bragg mirror micropattern appearing on the PVB film was the same as the PDMS stamp. Therefore, depending on the PDMS stamp, disk-shaped photonic crystals can be patterned either on the Si substrate or the PVB film. In the latter case, the polymer can be readily dissolved in an appropriate organic solvent resulting in a dispersion of disk-shaped PSi photonic crystals.

To verify the effectiveness of the micropatterning procedure, optical and structural characterization of a micropatterned PSi Bragg mirror were performed (Fig. 2). The optical image in Figure 2A shows the sharp color contrast between a

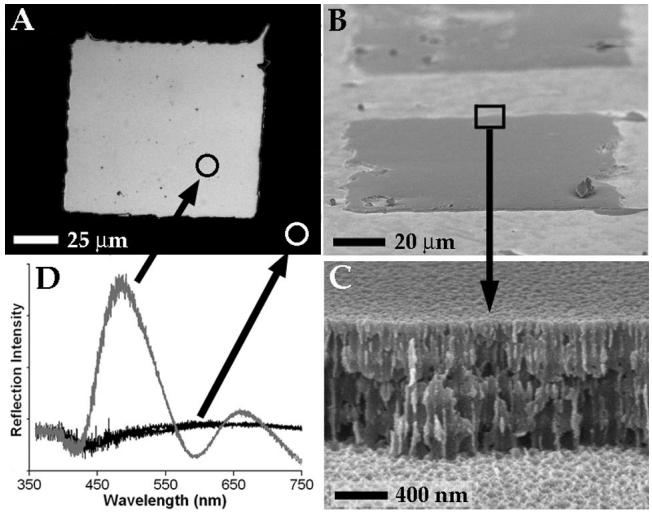

Figure 2. A) Contrast-enhanced optical image (top view) and B) SEM image (angled view) of 100 μm × 100 μm PSi Bragg mirror. C) Scanning electron microscope (SEM) cross-section image of Bragg mirror edge showing PSi layers. D) White-light reflectivity spectra collected from regions on the PSi Bragg mirror (gray) and Si substrate (black).

100 μm × 100 μm square-patterned PSi Bragg mirror and the surrounding Si substrate. Complete PSi Bragg mirror removal in the areas encompassing the micropatterned PSi Bragg mirror square was observed on the surrounding Si substrate. Additionally, the uniform color of the micropatterned PSi Bragg mirror square indicated preservation of the Bragg mirror layer structure throughout the patterning procedure. This was confirmed by electron microscopy, which showed the multilayer structure consisting of eight alternating layers of high- and low-porosity Si (Fig. 2C). These alternating layers, exhibited as light and dark layers, respectively, in the scanning electron microscope (SEM) image, had approximate thicknesses of 80 and 160 nm resulting in a total PSi Bragg mirror thickness of roughly 1 μm. Such thin Bragg mirror structures have the dimensional capability to be integrated with silicon processor architectures and could lead to more advanced optoelectronic devices.

ADVANCED MATERIALS

Spectral characterization by white-light reflectance spectroscopy, shown in Figure 2D, demonstrated the unique optical properties of the micropatterned PSi Bragg mirror. A reflectance spectrum collected from the surface of a micropatterned PSi Bragg mirror (gray curve) revealed a Bragg peak at approximately 486 nm. No change in Bragg peak position was observed after the micropatterning procedure. Reflectance spectra collected from the Si-substrate region, where PSi layers were removed by a PDMS stamp, exhibited no spectral features (black curve), confirming that the 1D photonic crystal had been removed. The remaining micropatterned platform consisted of uniform, optically functional microstructures that could be individually modified to enhance specific chemical detection. Therefore, we have shown that a single transfer step can be used to produce photonic-crystal arrays that can serve as the basis for a multiplexing sensor device.

Comparing the reflection spectra of a PSi Bragg mirror before and after transfer to a PVB film confirmed that the optical integrity of the PSi layers had been conserved throughout the transfer procedure from the Si substrate to the polymer film (Fig. 3). The reflection spectrum of the untouched Bragg mirror exhibited a Bragg peak at 514 nm (Fig. 3A), which, after transfer to a PVB film, shifted slightly to 522 nm

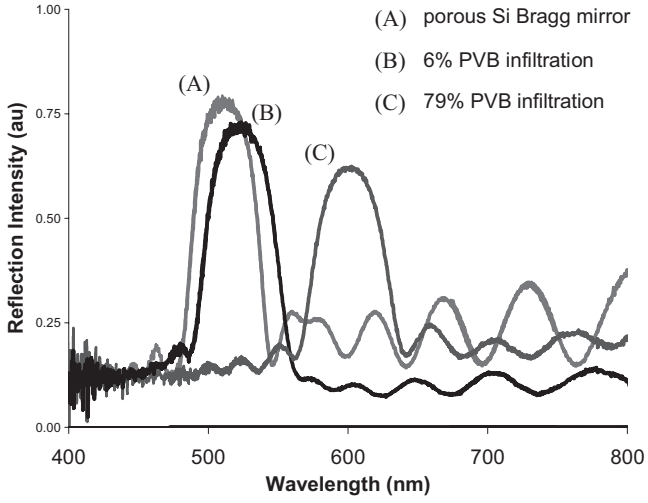

Figure 3. Reflection spectra showing PSi Bragg mirror optical properties before and after transfer to a PVB film. A) Untouched Bragg mirror, B) transfer to a PVB film with 6% PVB infiltration, C) transfer with 79% PVB infiltration.

(Fig. 3B). While the Bragg peak remained relatively unchanged after transfer to a PVB film, the intensity of the interference fringes along the baseline of the reflection spectrum was drastically reduced (Fig. 3B). This was due to the removal of the Si substrate, which eliminated the strong back reflection of the Fabry–Perot fringes of the Bragg mirror.

The shift in Bragg peak observed after transfer to a PVB film is due to the penetration of the PVB solution into the pores of the Bragg mirror during the transfer procedure. Since the refractive index of PVB ($n = 1.485$) is greater than that of air, the overall refractive index of the Bragg mirror increased as the PVB solution displaced the air inside the pores. Therefore, a red-shift of the Bragg peak was produced. Consequently, the amount of PVB solution applied to the Bragg mirror surface during the transfer procedure dictates the degree of spectral shift of the Bragg peak. Sparse application of the PVB solution (ca. 5 μL) minimized penetration of PVB into the pores of the PSi Bragg mirror, resulting in a small Bragg peak red-shift (Fig. 3B). On the other hand, heavy application of PVB solution (40–50 μL) allowed PVB saturation within the pores producing a large red-shift in Bragg peak (Fig. 3C).

Quantitative information about the volumetric infiltration of PVB into the pores of a PSi Bragg mirror can be estimated using the Bruggeman effective-medium approximation. The refractive index of the PSi Bragg mirror, before and after transfer to a PVB film, follows the form $n_{PSi} = \lambda/2d$, where n_{PSi} is the refractive index of PSi, λ is the Bragg peak wavelength, and d is the thickness of the period within the PSi Bragg mirror. Due to the fact that the periodic structure of the PSi Bragg mirror was composed of two separate layers of high- and low-porosity Si, in reality there existed two distinct refractive indices that changed as PVB infiltrated the PSi Bragg mirror. However, the two-layer period was approximated as a single domain, and therefore a single value for the refractive index of the PSi Bragg mirror, n_{PSi} was determined. This value, $n_{PSi} = 1.78$, was used to calculate the porosity of the PSi Bragg mirror using the Bruggeman effective-medium approximation[24] as shown by Equation 1

$$(1-f)\frac{\varepsilon_{Si}-\varepsilon_{PSi}}{\varepsilon_{Si}+2\varepsilon_{PSi}}+f\frac{\varepsilon_{air}-\varepsilon_{PSi}}{\varepsilon_{air}+2\varepsilon_{PSi}}=0 \quad (1)$$

where ε_{Si}, ε_{PSi}, and ε_{air} are the dielectric constants of Si, PSi, and air, respectively; f is the porosity of the dielectric medium; and the relation $n = \sqrt{\varepsilon}$ is used to convert the refractive index into the dielectric constant. Finally, the percentage of PVB within the pores was determined by substituting the refractive-index value of the PSi Bragg mirror after transfer to a PVB film and calculating the filling factor, f_{PVB}, of the PVB component

$$(1-f)\frac{\varepsilon_{Si}-\varepsilon_{PSi-PVB}}{\varepsilon_{Si}+2\varepsilon_{PSi-PVB}}+f_{air}\frac{\varepsilon_{air}-\varepsilon_{PSi-PVB}}{\varepsilon_{air}+2\varepsilon_{PSi-PVB}}+f_{PVB} \times\frac{\varepsilon_{PVB}-\varepsilon_{PSi-PVB}}{\varepsilon_{PVB}+2\varepsilon_{PSi-PVB}}=0 \quad (2)$$

where ε_{PVB} and $\varepsilon_{PSi-PVB}$ are the dielectric constants of PVB and PSi with PVB, respectively; f_{air} and f_{PVB} are the filling factors of air and PVB, respectively; and $f_{air}+f_{PVB} = f$. For an 8 nm Bragg peak red-shift (Fig. 3B), an increase in the PSi refractive index from 1.78 to 1.80 was determined. Assuming a refractive index of PVB of 1.485, an f_{PVB} of 4% was calcu-

lated using Equation 2. This indicated that 6 % of the air volume inside the PSi Bragg mirror had been replaced by the PVB polymer. Such small infiltration of the PVB polymer into the porous network of the PSi Bragg mirror was controlled by modest application of PVB during the transfer procedure. However, heavy application of the PVB polymer provided a more thorough infiltration of PVB polymer into the pores of the Bragg mirror resulting in a Bragg peak red-shift of 87 nm (Fig. 3C). This large shift in Bragg peak implied an increase in the PSi refractive index from 1.78 to 2.07, which resulted from PVB solution replacing 79 % of the air volume within the pores of the PSi Bragg mirror. These results compare favorably with prior studies on PSi microcavities in which shifts in peak wavelength were measured as a function of the liquid-layer fraction of various chemicals within the PSi microcavity.[6]

In addition, the effect of reversible chemical sensing via optical detection was demonstrated with a micropatterned PSi Bragg mirror (Fig. 4). The Bragg peak of a micropatterned Bragg mirror was red-shifted approximately 70 nm in the presence of an ethanol droplet as shown in Figure 4B. Using Equation 2, modified for ethanol instead of PVB, and inserting 1.359 as the refractive index of ethanol, the percentage of ethanol infiltration into the pores of the Bragg mirror was calculated to be 99 %, indicating complete pore saturation. This result was expected since the micropatterned Bragg mirror was encapsulated in a volatile-liquid environment. Most importantly, the reflection spectrum of the micropatterned Bragg mirror returned to its original form once the ethanol had evaporated, demonstrating a complete reversibility of the chemical sensor.

We have developed a simple, cost-effective method for patterning PSi Bragg mirrors into virtually any desired shape using micropatterned PDMS-elastomer stamps. Through a single transfer step we can fabricate arrays of optically functional PSi Bragg mirror microstructures on both silicon and polymer platforms. The optical integrity of the films after transfer exhibited no noticeable degradation, verifying the delicacy of the dry-removal technique. In addition, quantifiable chemical detection using simple reflectance spectroscopy was demonstrated with a polymer via pore infiltration. These nanostructured materials utilize a mechanism for chemical detection that is completely reversible, and can not only be used for conventional gas sensing via condensation in the pores, but also for sensing liquids via air replacement. With the capability of transferring the photonic crystals directly to a flexible freestanding polymer film, we open up the potential for mass-producing chemically addressable pixels for high-selectivity and high-throughput sensing in chemical- and biochip applications.

Experimental

Porous silicon (PSi) Bragg mirrors were prepared by anodically etching a p-type silicon wafer (B-doped, (100)-oriented, 0.01 Ω-cm resistivity, University Wafer) in a Teflon electrochemical cell [25]. The etchant consisted of 48 % aqueous HF/ethanol (1:2 by volume). The high- and low-porosity layers were constructed by applying alternating currents of 9 and 21 mA cm^{-2} with 12.5 s layer^{-1} etch times (100 s total etch time). Removal of the PSi film from the substrate was aided by a short electropolishing pulse (75 mA cm^{-2} for 2 s) at the end of the etch. The samples were rinsed with ethanol and dried with nitrogen gas.

Reflectivity data were collected using a reflection/backscattering probe (Ocean Optics Inc., Model R400-7) coupled to a bifurcated fiber-optic cable. Illumination of the sample was achieved through a central fiber by a tungsten-filament light source and the reflected light was carried by the six surrounding fibers to a charge-coupled device (CCD) spectrometer (Acton Research Corporation, SpectraPro 150).

The micropatterning procedure was carried out by placing a prepatterned polydimethylsiloxane (PDMS)-elastomer stamp (10:1 by weight, Dow Corning, 184 elastomer kit) on the top surface of a PSi Bragg mirror with a slight applied pressure (a 50 g weight) and mechanically removing the stamp after 5 min. To transfer the PSi residing on the PDMS to a freestanding polymer film, a solution of (poly[(vinyl butyral)-*co*-(vinyl alcohol)-*co*-(vinyl acetate)] (PVB) in ethanol) was drop-cast on the stamp and allowed to cure for 24 h. To minimize infiltration of PVB into the pores of the PSi Bragg mirror, and thus minimize Bragg peak red-shift, the PVB solution was allowed to cure for a few minutes before application to the Bragg mirror surface. Once dry the PVB film was peeled off the stamp, removing the PSi Bragg mirror pattern from the stamp surface. Surface images of patterned PSi Bragg mirrors were captured with an optical microscope (Nikon) under diffuse illumination (bright field). Higher resolution images were obtained using a scanning electron microscope (JEOL 6300F SEM operating at 5 kV accelerating voltage).

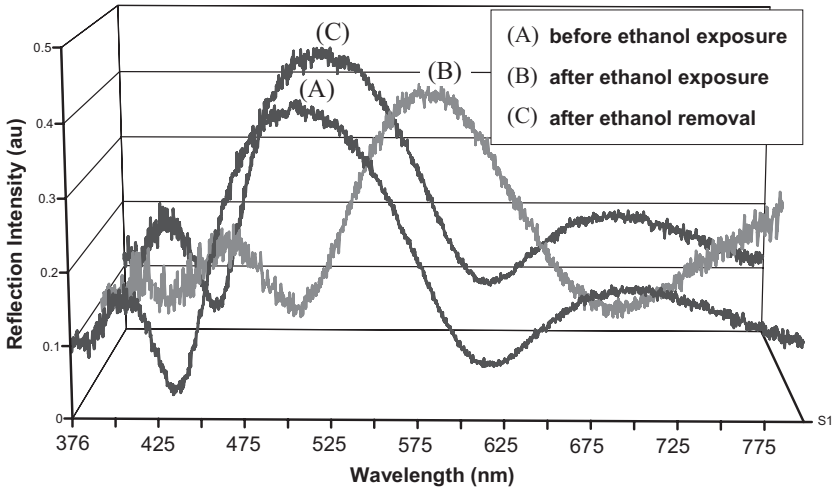

Figure 4. Micropatterned PSi Bragg mirror demonstrating optical detection of ethanol. A) Reflection spectrum of micropatterned Bragg mirror, B) after ethanol exposure, C) after ethanol removal.

Received: July 19, 2006
Revised: August 30, 2006
Published online: November 10, 2006

[1] M. G. Berger, C. Dieker, M. Thonissen, L. Vescan, H. Luth, H. Munder, W. Theiss, M. Wernke, P. Grosse. *J. Phys. D: Appl. Phys.* **1994**, *27*, 1333.
[2] G. Vincent. *Appl. Phys. Lett.* **1994**, *64*, 2367.
[3] S. Frohnhoff, M. G. Berger. *Adv. Mater.* **1994**, *6*, 963.
[4] C. Mazzoleni, L. Pavesi. *Appl. Phys. Lett.* **1995**, *67*, 2983.
[5] C. Baratto, G. Faglia, G. Sberveglieri, Z. Gaburro, L. Pancheri, C. Oton, L. Pavesi. *Sensors* **2002**, *2*, 121.
[6] L. De Stefano, N. Rendina, L. Moretti, S. Tundo, A. M. Rossi. *Appl. Opt.* **2004**, *43*, 167.
[7] J. Dorvee, M. J. Sailor. *Phys. Stat. Solidi A: Appl. Mater. Sci.* **2005**, *202*, 1619.
[8] A. Loni, L. T. Canham, M. G. Berger, R. Arens-Fischer, H. Munder, H. Luth, H. F. Arrand, T. M. Benson. *Thin Solid Films* **1996**, *276*, 143.
[9] P. J. Reece, G. Lerondel, W. H. Zheng, M. Gal. *Appl. Phys. Lett.* **2002**, *81*, 4895.
[10] S. M. Weiss, P. M. Fauchet. *Phys. Stat. Solidi A: Appl. Mater. Sci.* **2003**, *197*, 556.
[11] E. Lorenzo, C. J. Oton, N. E. Capuj, M. Ghulinyan, D. Navarro-Urrios, Z. Gaburro, L. Pavesi. *Appl. Opt.* **2005**, *44*, 5415.
[12] J. Diener, N. Kunzner, E. Gross, D. Kovalev, M. Fujii. *Phys. Stat. Solidi A: Appl. Mater. Sci.* **2005**, *202*, 1432.
[13] S. Chan, P. M. Fauchet, Y. Li, L. J. Rothberg, B. L. Miller. *Phys. Stat. Solidi A: Appl. Mater. Sci.* **2000**, *182*, 541.
[14] J. Volk, J. Balazs, A. L. Toth, I. Barsony. *Sens. Actuators, B* **2004**, *100*, 163.
[15] L. Rotiroti, L. De Stefano, N. Rendina, L. Moretti, A. M. Rossi, A. Piccolo. *Biosens. Bioelectron.* **2005**, *20*, 2136.
[16] M. J. Sailor, J. R. Link. *Chem. Comm.* **2005**, 1375.
[17] F. Cunin, T. A. Schmedake, J. R. Link, Y. Y. Li, J. Koh, S. N. Bhatia, M. J. Sailor. *Nat. Mater.* **2002**, *1*, 39.
[18] Y. Y. Li, V. S. Kollengode, M. J. Sailor. *Adv. Mater.* **2005**, *17*, 1249.
[19] Y. N. Xia, G. M. Whitesides. *Annu. Rev. Mater. Sci.* **1998**, *28*, 153.
[20] D. C. Duffy, R. J. Jackman, K. M. Vaeth, K. F. Jensen, G. M. Whitesides. *Adv. Mater.* **1999**, *11*, 546.
[21] Y. D. Yin, B. Gates, Y. N. Xia. *Adv. Mater.* **2000**, *12*, 1426.
[22] D. J. Sirbuly, G. M. Lowman, B. Scott, G. D. Stucky, S. K. Buratto, *Adv. Mater.* **2003**, *15*, 149.
[23] Y. Y. Li, P. Kim, M. J. Sailor. *Phys. Status. Solidi A: Appl. Mater. Sci.* **2005**, *202*, 1616.
[24] W. Theiss. *Adv. Solid State Phys.* **1994**, *33*, 149.
[25] M. D. Mason, D. J. Sirbuly, S. K. Buratto. *Thin Solid Films* **2000**, *406*, 151.

